Journal of Engineering Science and Technology
Vol. 20, No. 6 (2025) 2154 - 2171

COMPUTATIONAL ANALYSIS OF INTEGRAL FINED TUBE WITH DIFFERENT PITCH RATIO TO IMPROVE CROSSFLOW HEAT EXCHANGER PERFORMANCE

MOHAMMED K. JAR[1,*], KAMIL ARSLANE[1], ZENA K. KADHIM[2]

[1]Mechanical Engineering Department, Karabük University, Karabük, Turkey
[2]Mechanical Engineering Department, College of Engineering, Wasit University, Iraq
*Corresponding Author: drzena@uowasit.edu.iq

Abstract

Fin spacing, which promotes heat exchange in heat exchangers, is not evaluated using various flow parameters. This study deals with medium integral finned tubes with variable pitches to get the optimum amount of heat transfer numerically. Four pipes with a length of 250 mm for each tube have been modelled and simulated with water flow inside the tubes and air flow over the tubes. The smooth model served as the baseline for comparison with three finned tube models featuring fin pitches of 1.6 mm, 2.5 mm, and 3.75 mm. The designs were developed using SolidWorks 2018, and simulations were conducted with ANSYS Fluent 19R2. By using water as a working fluid in pipes with different flow rates of 2, 3, 4, 5, and 6 L/min, and air-cooled flow, across the tubes with velocities of 1, 2, 3, and 4 m/s have been tested with inlet water temperatures of 50, 60, 70 ºC and 20 ºC for inlet air. Variations of water and air velocity magnitudes and inlet temperature on convective heat transfer characteristics have been determined to be 68.1%, 73.5%, and 80.4% for the pitches of 3.75, 2.5, and 1.6 mm, respectively. The results indicate that reducing the fin pitch leads to an increase in the number of fins, hence increasing the surface area available for heat exchange. Consequently, this enhances the rate of heat transfer.

Keywords: CFD, Crossflow heat exchanger, Heat transfer, Integral finned tube, Pitch ratio.

1. Introduction

Heat transfer improvement in a finned tube is not only wide but also significant in industries, including the petrochemical industry, waste heat recovery, power plant boilers, and wood drying, as it works to enhance the heat transfer rate by increasing the external surface area. Many researchers have studied the types of fins and how to improve their performance.

Mon and Gross [1] studied the effect of fin spacing on an inline and staggered tube bundle with the bundle pitch varying between 1.6, 2, and 4 mm, constant fin height of 5 mm, and a diameter of 24 mm. At the front of the fins and the end of the fin base, they were able to find boundary layers. Both configurations even exhibited a growth in the aspect ratio of the heat transfer coefficient. To enhance the performance of a heat exchanger under crossflow conditions, Hofmann et al. [2] performed experimental tests on a tube with finned heat exchangers such as serrated, stiff, and cross-sectional fins to assess the heat transfer and pressure flux. The findings indicated the disparity between the rigid and threaded finned tubes.

Jung and Assanis [3] developed a predictive numerical model for finned crossflow heat exchangers, focusing on total transfer rate and airflow resistance. They evaluated performance in two cases, finding that increasing the cooler core dimensions by 8% increases the heat expulsion rate. Taher [4] examined the heat transfer of crossflows in heat exchangers, where he evaluated four air-cooled heat exchangers with air flowing in at a velocity of 1, 1.7, and 2.3 m/s, water flowing at 2-6 LPM, and varying temperatures up to 70 °C. The researchers discovered that an increase in air velocity and water entry temperature amplifies the heat transfer. The Finned tubes performed much better than the smooth tube, with the greatest performance being in the tube with many fins. The best improvement in the heat transfer over the smooth tube with respect to low, medium, and high fins was 50%, 203.9% and 329.9%, respectively.

Wais's study [5] on fluid flow in a heat exchanger with radial fins (2.6 mm spacing and 80 mm tube diameter) assumed no resistance between the fin base and tube surface. The three models tested were in air inlet velocities of 0.5, 1, and 1.5 m/s, air temperature 10 °C, and liquid inlet temperature 90 °C. The third model proved most effective, and the optimum velocity of the air turned out to be 1 m/s.

The study carried out by Ismail et al. [6] simulated in three dimensions the design of a crossflow heat exchanger using air as external flow, between 1 and 6 m/s velocity, and hot water as a laminar internal flow that had a Re of 1,200. They found that the smaller tube by 1 mm outperformed the larger one of 10 mm, increasing heat flow per unit volume by 20% as airspeed rose. Fin efficiency ranged from 97% to 91% for the 10 mm tube and 99.98% to 99.99% for the 1 mm tube. Fins proved effective in normal exchanges but not useful in smaller ones.

Merdan and Khalefa Kadhim [7] examined the effects of multiple tubes and flow directions on heat transfer in a crossflow heat exchanger. They tested five smooth copper tube models with a constant flow of 5 LPM and pipe outer diameters and inner diameters of 24 and 19 mm, respectively. Cold and hot liquid temperatures were set at 25 and 80 °C. Heat transfer increased with tube length, but at the expense of a higher pressure drop. A triangular finned tube model showed superior heat transfer, with the 4-pipe model offering the best balance for efficiency. Wais [8] evaluated air-side connections in a heat exchanger, analysing heat transfer in a tube and fin exchanger

with varying fin thicknesses. At an air inlet velocity of 4 m/s, a fluid temperature at the inlet of 300 °C, and a temperature at the tube surface of 70 °C, 3D models showed that thicker fins reduced heat transfer. The computational results aligned with experimental data, accurately predicting heat transport coefficients.

Ravikumar et al. [9] implemented ANSYS Fluent 15.0 to investigate the heat transfer in a heat exchanger with smooth and finned tubes. With the hot water inside and ambient air cool outside, the model investigated an air flow rate of 4 m/s, temperature at liquid inlet 300 °C, and temperature at tube surface 70 °C. The results showed a higher temperature gradient in the finned tube, emphasising the fin's role in enhancing temperature differences within the tube. Taher and Kadhim [10] analysed an eight-pass copper tube heat exchanger with fin heights of 1.5 mm and 3 mm. Tests were conducted using air velocities between 1 and 4 m/s, water flow rates from 2 to 6 LPM, and fluid temperatures ranging from 50 to 80 °C. The 3 mm fins increased heat transfer by 15%, showed a larger temperature gradient, and reduced water outlet temperature compared to the 1.5 mm fins and smooth tubes.

On the other hand, Sahel et al. [11] empirically investigated the influence of tube geometry on thermal energy transfer in a heat exchanger. Various tube shapes (circular, flat, and oval) were compared using simulations with Reynolds numbers from 3,000 to 20,000. The results showed that tube geometry significantly affects thermal and dynamic characteristics, with elliptical tubes yielding the lowest pressure losses. Merdan and Kadhim [12] studied crossflow heat exchangers with four fined smooth tubes, using circular and triangular fins on 25 cm tubes at flow rates of 2-5 L/min, air speeds of 1-3 m/s, and inlet temperatures of 50 - 80 °C. ANSYS and SolidWorks were used to analyse heat transfer with Reynolds numbers from 4,022 to 50,194. The optimal tube length was 2.5 m, achieving a heat transfer rate of 654.6 W, though the pressure drop increased to 651 Pa. Circular fins with rectangular cross-sections provided the best heat transfer rate at 32.98%, with no impact from flow direction.

Kadhim et al. [13] were researching the topic of heat transfer intensification in a crossflow heat exchanger in relation to a low-fin tube. They compared a smooth 19 mm inner diameter, 24 mm outer diameter copper tube to a finned 19 mm inner diameter, 21 mm root, and 1.5 mm high tube. Airflow ranged from 1 to 6 LPM, with water inlet temperatures of 50-80 °C. The finned tube improved heat dissipation by 72% over the smooth tube due to increased cooling surface area and better boundary layer penetration. Kadhim et al. [14] numerically studied low-integral finned pipes in a crossflow heat exchanger using SOLIDWORKS Premium 2013. An 8-pass copper tube (19 mm inner, 21 mm root, 24 mm outer diameter) with 1.5 mm fins was placed in a 1200 mm air duct. Air velocities ranged from 1 to 4 L/sec, with water flow rates of 2 to 6 L/min and inflow temperatures of 50 °C to 80 °C. The findings indicated that the low-finned tube had a better heat transfer coefficient and temperature difference in comparison with the smooth tube.

Nuntaphand and Kiatsiriroat [15] investigated fly ash residuals and their implications on the performance of a spiral finned tubes crossflow heat exchanger. Warm air at 40 °C containing fly ash exchanged heat with cold water at 5 °C, flowing at 10 L/min. Over time, ash buildup increased thermal resistance, reducing heat transfer efficiency. The ash deposition was influenced by ash content, condensate, fin quality, geometry, and fin pitch. Habeeb et al. [16] experimentally studied heat transfer in a crossflow, multiple pass, air-cooled aluminium tube with low fins. Air velocities of 1, 2, and 3 m/s, water flow at 5 L/min, and hot fluid temperatures of 50 °C to 80 °C were tested. The low-finned tube improved heat

transfer by 1.86 to 2.38 times compared to a smooth tube, with higher air speeds further enhancing the external heat transfer coefficient.

Because of the widespread use of heat exchangers in industrial practice, it is normal to want to seek an increase in their thermal efficiency. In line with this, the current research is aimed at the optimisation of crossflow heat exchangers via determining an optimum pitch ratio of the finned tubes to attain a higher heat transfer rate. The gain that is realised is owing to the high temperatures of the heat transfer coefficients that are maintained because of the use of finned tubes that have different pitches. The current study also used ANSYS Fluent 19.2 R2 to model finned tubes with varying pitch ratios, identifying the optimal pitch for maximising heat transfer compared to smooth tubes and previous research.

2. Computational Implementations

This computational process tries to calculate and establish the optimal pitch fins within the crossflow heat exchanger tube and contrasts the same between different models using a four-pass crossflow heat exchanger. Accordingly, a model has been developed and meshed, and a set of governing equations has been solved using ANSYS Fluent 19.2R2.

2.1. Model generation

The entire test section is shown in Fig. 1, with overall dimensions of 250 mm width, 375 mm height, and 400 mm length in the air flow direction. With the help of Solid Works 2018 and ANSYS Fluent 19.2 R2 preparation of the crossflow type of heat exchanger and adjacent component.

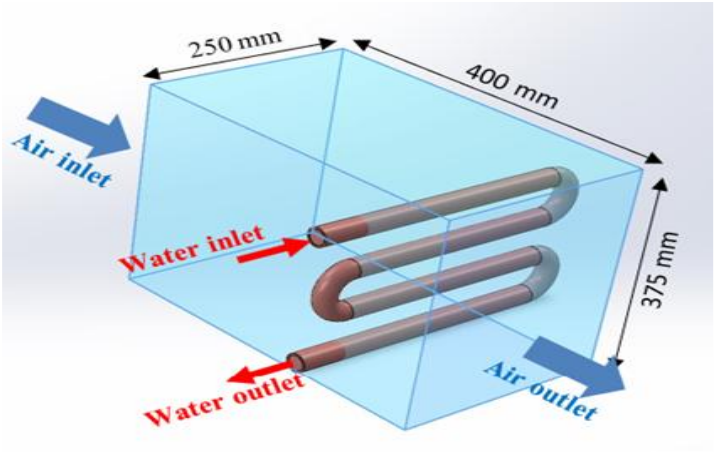

Fig. 1. Air zone shape and size of the heat exchanger.

2.1.1. Air zone

The entire domain of this part is biggest computation area of this model, and it is 800 mm, 250 mm and 275 mm in length, width and height respectively as shown in Fig. 1. Its outer surface is in the contact with the air so it could receive the process of heat exchange and be isolated with the outside which lacks the radiation and heat generation.

2.1.2. Pipes

This section is a test section, and this is the most significant part of the work. As Fig. 2 shows, the test section is composed of four passages, a tube with a diameter of 19 mm through which hot water flowing through it. Outside diameter 21 mm, whereby when passing air, it comes into contact with the outside of the corridor, and the length is 250 mm in one corridor. Three sets of pipe models with fin pitches of 1.6 mm, 2.5 mm, and 3.75 mm have been generated. Also, one model with a smooth pipe has been generated and used as a bare case for the evaluation of the heat exchanger enhancements. In the case of the finned tube, the external diameter amounts to 28.5 mm.

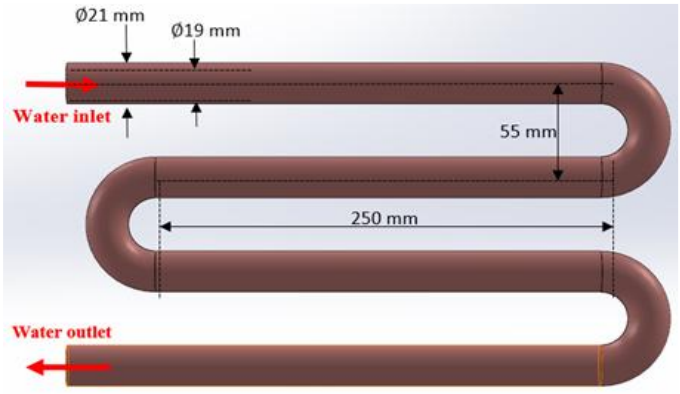

Fig. 2. The size of the tube opening of the study.

2.1.3. Fins

The smooth tube is made of fins. In the process of making the surface area larger, its heat transfer rate rises. The creation of these fins has been conducted with the software SolidWorks 2018. Fins are circular and cross-section rectangular shaped with a height of 3.75 mm, a width of 1 mm, and a pitch of 1.6 mm between them, and it is represented in Fig. 3.

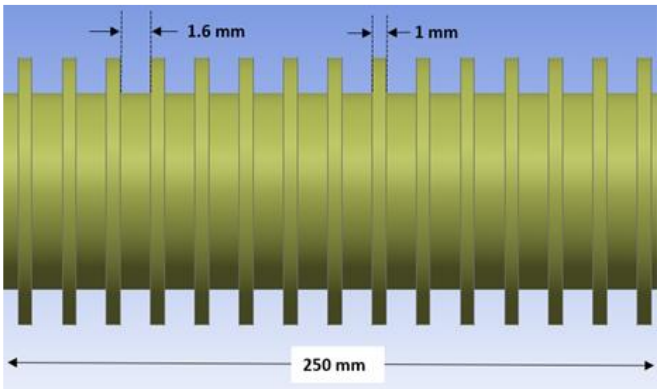

Fig. 3. Fins dimensions.

Three finned tubes were used with different numbers of fins. Various pitch ratios have been applied in order to come up with the optimum ideal case in which the best heat transfer rate is achieved. Fin pitches of 1.6, 2.5, and 3.75 mm were considered in the investigation. The selected pitches led to 380, 284, and 212 fins, respectively, as indicated in Fig. 4.

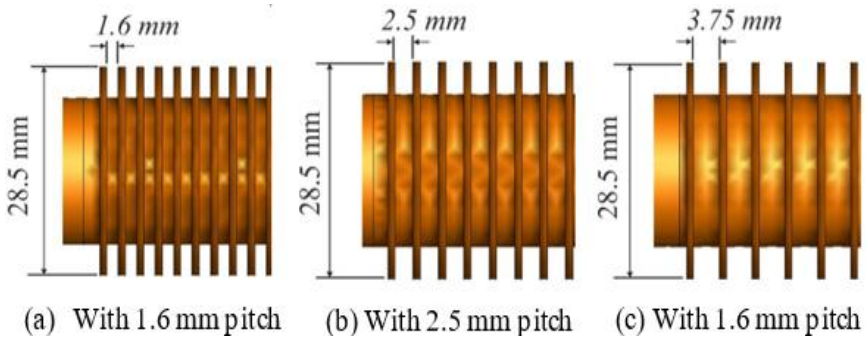

Fig. 4. The fined tube geometries of the test models.
(a) with 1.6 mm pitch, (b) with 2.5 mm Pitch, and (c) with 3.75 mm pitch.

2.2. Boundary conditions

The flow rates of water have been between 2 and 6 l/min at the inlet temperatures of 50, 60, and 70 ºC as Table 1 indicates. Air velocity will be 1, 2, 3, and 4 m/s with the temperature at the inlet of 20 ºC. Reynolds numbers of flow of water have been changed within a range of $3985 < Re_w < 16032$, and airflow has been changed within a range of $17390 < Re_a < 73060$.

Table 1. Conditions of the boundary

Air boundary condition at the inlet	
Temperature	20 ºC
Velocities at the inlet	1, 2, 3, 4 m/s
Turbulent intensity	4%
Hydraulic diameter	261.9 mm
Air boundary condition at the outlet	
Outlet pressure	0 (Pa)
Turbulence intensity	4%
Hydraulic diameter	262 mm
Water boundary conditions at the inlet	
Temperature	70 ºC
flow rate	2, 3, 4, 5, and 6 LPM
Turbulence intensity	5%
Hydraulic diameter	19 mm
Water boundary condition at the outlet	
Outlet pressure	0 Pa
Boundary condition for the tube wall	
Thermal condition	Coupled
Wall shear condition	No slip

2.3. Governing equations

The results have been derived with the help of governing equations to achieve the optimal model of the research. Such equations are the conservation of mass, momentum, and energy equations with suitable turbulence modelling equations. The reason for selecting energy equation and viscous k-epsilon, RNG, Standard wall functions was that they can represent the placement of one more equation of *k*-epsilon to develop the correctness of the slowly cleaned flows and enhance the accuracy of the flows of eddy because they are most used in tube flow to solve the multifaceted issue of turbulent and fast speed. To solve these equations, some assumptions should be made: three-dimensional analysis, turbulent flow, steady state, incompressible fluid, constant physical properties of the fluid, and adiabatic walls of the pipe (elbow). Depending on the previous literature, the recommendations of [4, 10, 17-19] have been used in the solution in this study.

Conservation of Mass:

$$\frac{\partial \bar{\mathrm{u}}}{\partial \mathrm{x}}+\frac{\partial \bar{\mathrm{v}}}{\partial \mathrm{y}}+\frac{\partial \bar{\mathrm{w}}}{\partial \mathrm{z}}=0 \tag{1}$$

Conservation of Momentum:

$$\left(\bar{u}\frac{\partial \bar{u}}{\partial x}+\bar{v}\frac{\partial \bar{u}}{\partial y}+\bar{w}\frac{\partial \bar{u}}{\partial z}\right)+\left(\frac{\partial}{\partial x}\left(\overline{u'^2}\right)+\frac{\partial}{\partial y}\left(\overline{u'v'}\right)+\frac{\partial}{\partial z}\left(\overline{u'w'}\right)\right)=-\frac{1}{\rho}\frac{\partial P}{\partial x}+\frac{\mu}{\rho}\left(\frac{\partial^2 \bar{u}}{\partial x^2}+\frac{\partial^2 \bar{u}}{\partial y^2}+\frac{\partial^2 \bar{u}}{\partial z^2}\right) \tag{2}$$

$$\left(\bar{u}\frac{\partial \bar{v}}{\partial x}+\bar{v}\frac{\partial \bar{v}}{\partial y}+\bar{w}\frac{\partial \bar{v}}{\partial z}\right)+\left(\frac{\partial}{\partial x}\left(\overline{u'v'}\right)+\frac{\partial}{\partial y}\left(\overline{v'^2}\right)+\frac{\partial}{\partial z}\left(\overline{u'w'}\right)\right)=-\frac{1}{\rho}\frac{\partial P}{\partial y}+\frac{\mu}{\rho}\left(\frac{\partial^2 \bar{v}}{\partial x^2}+\frac{\partial^2 \bar{v}}{\partial y^2}+\frac{\partial^2 \bar{v}}{\partial z^2}\right) \tag{3}$$

$$\left(\bar{u}\frac{\partial \bar{w}}{\partial x}+\bar{v}\frac{\partial \bar{w}}{\partial y}+\bar{w}\frac{\partial \bar{w}}{\partial z}\right)+\left(\frac{\partial}{\partial x}\left(\overline{u'w'}\right)+\frac{\partial}{\partial y}\left(\overline{uv'}\right)+\frac{\partial}{\partial z}\left(\overline{w'^2}\right)\right)=-\frac{1}{\rho}\frac{\partial P}{\partial z}+\frac{\mu}{\rho}\left(\frac{\partial^2 \bar{w}}{\partial x^2}+\frac{\partial^2 \bar{w}}{\partial y^2}+\frac{\partial^2 \bar{w}}{\partial z^2}\right) \tag{4}$$

Conservation of Energy:

$$\left(\bar{u}\frac{\partial \bar{T}}{\partial x}+\bar{v}\frac{\partial \bar{T}}{\partial y}+\bar{w}\frac{\partial \bar{T}}{\partial z}\right)+\left(\frac{\partial}{\partial x}\left(\overline{u'T'}\right)+\frac{\partial}{\partial y}\left(\overline{v'T'}\right)+\frac{\partial}{\partial z}\left(\overline{w'T'}\right)\right)=\alpha\left(\frac{\partial^2 \bar{T}}{\partial x^2}+\frac{\partial^2 \bar{T}}{\partial y^2}+\frac{\partial^2 \bar{T}}{\partial z^2}\right) \tag{5}$$

Dissipation Rate (ε) Equation

$$\rho\left(\bar{u}\frac{\partial \epsilon}{\partial x}+\bar{v}\frac{\partial \epsilon}{\partial y}+\bar{w}\frac{\partial \epsilon}{\partial z}\right)=\left[\left(\mu+\frac{\mu_t}{\sigma_{\epsilon\epsilon}}\right).\left(\frac{\partial^2 \epsilon}{\partial x^2}+\frac{\partial^2 \epsilon}{\partial y^2}+\frac{\partial^2 \epsilon}{\partial z^2}\right)\right]+C_{1\epsilon}\frac{\epsilon}{k}G_k-C_{2\epsilon}\rho\frac{\epsilon}{k}] \tag{6}$$

The Eddy Viscosity of Turbulent:

$$\mu_t=\rho C_\mu\frac{K^2}{\epsilon} \tag{7}$$

The ratio of fluctuations, $\acute{u}$, to the average velocity, u_{ave}, is called turbulence intensity, T.I. It varies with Re and could be obtained from Eq. (8) [19]:

$$\mathrm{T.I.}=0.16\times(Re)^{(-1/8)} \tag{8}$$

The turbulent intensity is 4%, and the hydraulic diameter is 261.9 mm for air. For water, the turbulent intensity is 5%, and the inner diameter is 19 mm.

2.4. Mesh generation

The generation of mesh was also carried out using Gambit 2.4.6 software, which offers the best preparation in determining the aspects of entry and exit of hot fluid and cold pipe walls and boundary turbulence of the working fluids. Subsequently, the geometry is exported to the ANSYS Fluent 19R2 program.

ANSYS offers various models, and such models are those that dictate the kind of object being determined, the size of the meshing to be formed, the number of nodes formed in the body, and the precision that will be acquired. Because the model employed in current research is complex and is also of a small size, it is intended that the number of cells used would be large, because the larger the number of cells, the more accuracy, although this will require much time to obtain the results. An additional number of possibilities to establish the accuracy and efficiency of the simulation and its influence on the stability of viscous flows and mesh quality are available [19]. The results scheme of the model meshing is shown in Figs. 5 and 6, and the mesh specifications are detailed in Table 2.

Fig. 5. Mesh shape for the smooth tube.

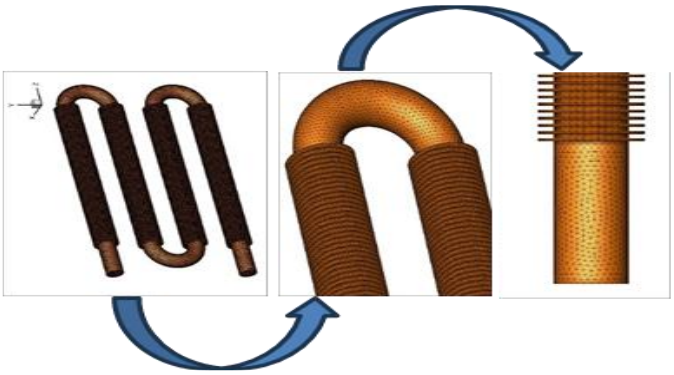

Fig. 6. Mesh for the finned tube.

Table 2. Meshes specifications.

Setup	Specifications

	Smooth Pipe	Fined Pipe
Physics Preference	CFD	CFD
Solver Preference	ANSYS Fluent 19R2	ANSYS Fluent 19R2
Growth Rate	Default (1.2)	Default (1.2)
Sizing	Fine mesh	Fine mesh
Max Skewness	0.902	0.913
No. of Nodes	813,167	985,850
No. of Elements	4,481,282	4,975,702
Transition	Slow	Slow
The Shape of The Mesh	The structure of the computational grid is Tetrahedral	The structure of the computational grid is Tetrahedral

2.5. Independence of Mesh

A grid independence test is significant in the dependability of the mesh. The net that is used in this paper is also analysed by varying the parameters and rerunning the work of simulation in order to check the correctness of the answers that are obtained. The primary aspect employed in this test was the increment of the elements of the pipe until a point where the outcome becomes insignificant. Figures 7, 8 and Tables 3 and 4 show that the change in temperature is not very significant as the number of elements increased. The best mesh sizes selected are 4,481,282 and 4,975,702 for smooth tube and finned tube, respectively, with pitch of 1.6 mm, and it takes a shorter time to calculate.

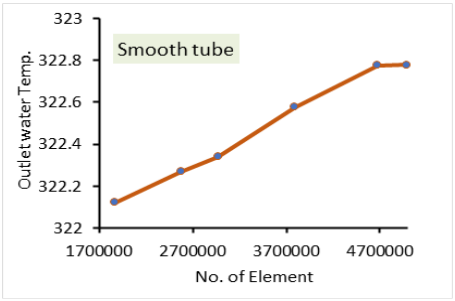

Fig. 7. Smooth tube mesh independence.

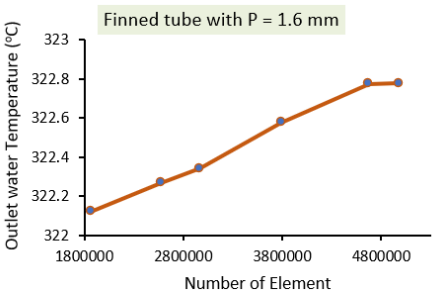

Fig. 8. Mesh independence for finned tube with pitch fin, P = 1.6 mm.

Table 3. Mesh independence for a smooth tube.

Elements	Nodes	Outlet water	% of

		temperature	difference
1,765,720	299,368	322.122	
2,438,392	362,415	322.268	0.068
2,708,849	420,598	322.341	0.032
3,652,275	634,257	322.578	0.101
4,481,282	813,167	322.775	0.076
4,625,561	897,263	322.778	0.001

Table 4. Finned tube mesh independence, P = 1.6 mm.

Elements	Nodes	Outlet water temperature	% of difference
1,865,422	299,368	321.128	
2,574,317	362,415	321.245	0.103
2,967,542	420,598	321.377	0.106
3,788,971	634,257	321.478	0.073
4,975,702	985,850	321.597	0.080
4,981,312	1,081,544	321.599	0.001

3. Results and Discussion

3.1. Validation

The computational procedure is validated by comparison of the results with [12]. The same values are obtained with a slight variance because the researcher in [12] considered the temperature of air to be 25 ºC, whereas in this study it was taken as 20 ºC. Here, it can be discussed that the program is accurate as stated in Fig. 9 and Table 5, which describes the comparison of the two studies.

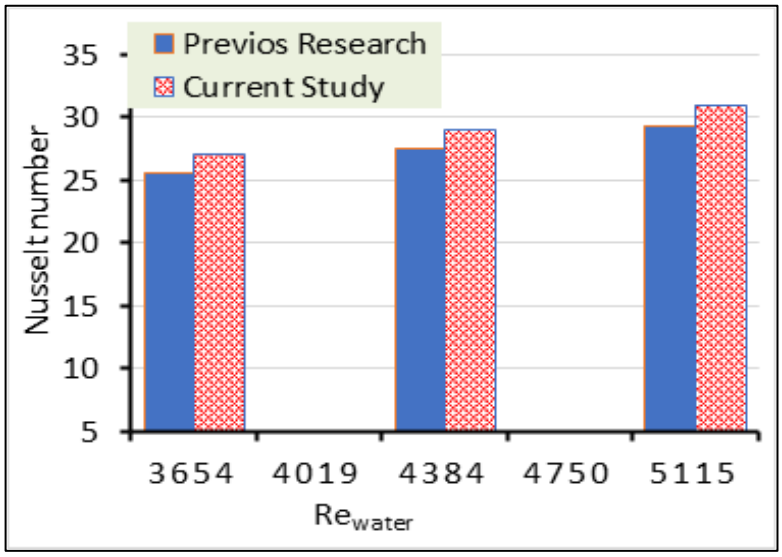

Fig. 9. Comparing the Nusselt number versus the Reynolds number between the current study and the Previous study [12].

Table 5. The comparison between this study and the study of Mardan [12].

Variable	Mardan [12]	Present simulation
	Input variables	
U_{air} m/s	1	1
$\dot{m}_w$ kg/s	0.033	0.033
T_{hi} ^{O}C	50	50
T_{ci} ^{O}C	25	20
	Output variables	
T_{ho} ^{O}C	49.56	49.61
T_{co} ^{O}C	25.73	21.86
ΔT_w ^{O}C	0.438	0.393
ΔT_a ^{O}C	0.725	1.88
Q_w Watt	60.34	54.05

3.2. Fins' effect on heat transfer

The results obtained through the study are for three integral finned tube models, with a pitch ratio of 1.6, 2.5, and 3.75 mm, and a smooth tube model. The finned tubes improve the heat transfer rate in general compared to smooth tubes for all pitch ratios, as shown in Fig. 10. In addition, the amount of thermal energy transferred increases with increasing inlet temperature for all models. The data indicate that the finned tube with an aspect ratio of 1.6 has the highest value of heat transfer rate compared to other models, and the discontinuous thermal boundary layer makes it the best despite the fact that most of the surface area is increased. Such behaviour could be attributed to the equal distribution of air on the surface of the tube; further vortexes generated behind the tube pierce the layer of this boundary, and this led to the decrease of the thermal resistance and the increase of the heat transfer.

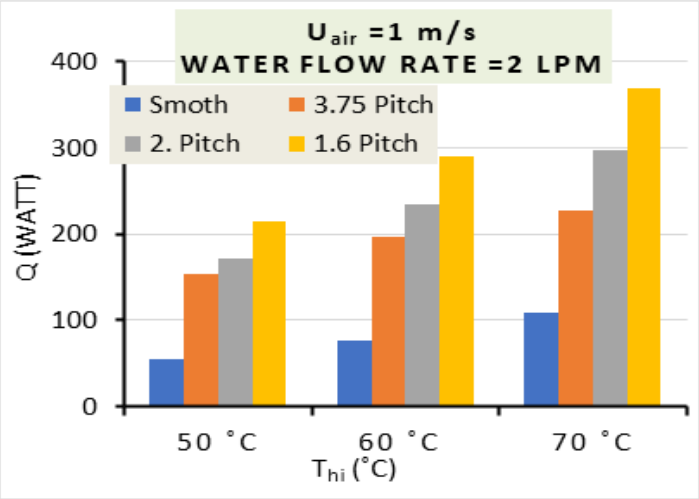

Fig. 10. The effect of inlet water temperature on the heat transfer rate from smooth tubes and finned tubes with different pitch ratios.

3.3. Temperature distribution for finned tube

The cooling tubes applied in this study are a smooth tube model, a thin finned tube model with a pitch ratio of 1.6, 2.5, and 3.75 mm, respectively, as shown in Figs. 11-14. It indicates the amount of air distribution that overflows the

pipes on the air side. By comparison of values, it is evident that there is a progressive stretch in temperature as the cross-sections of conduits 1, 2, 3, and 4 are allowed to cool.

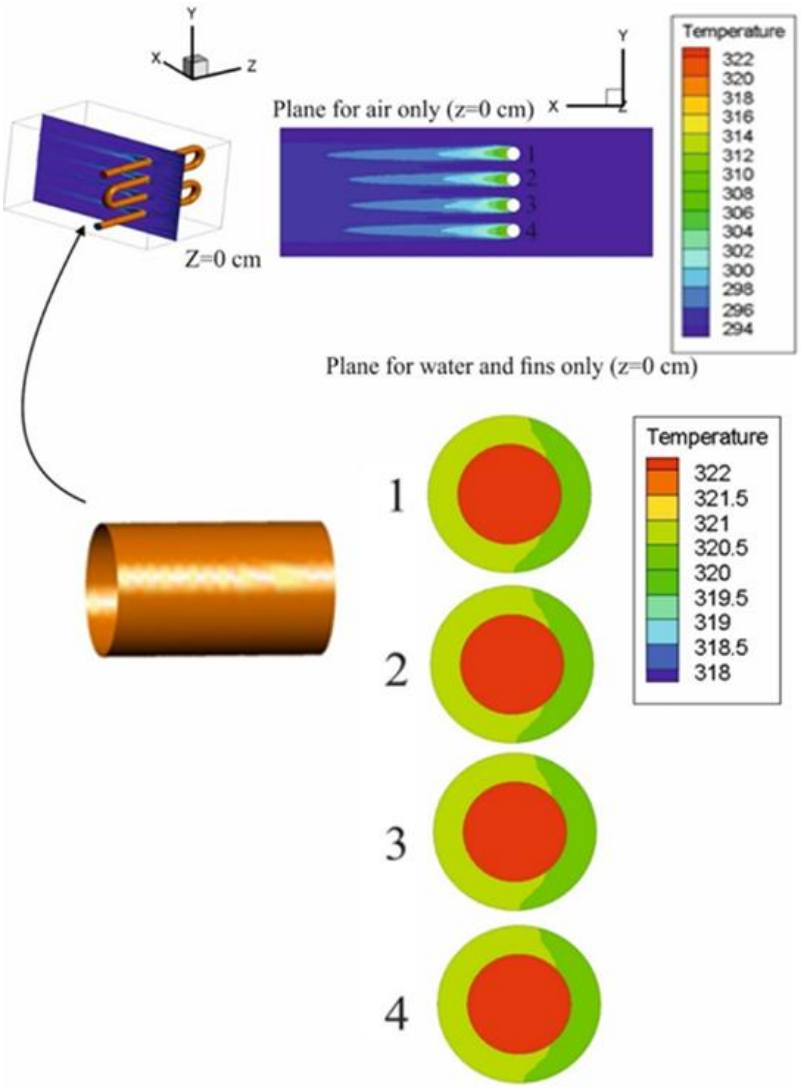

Fig. 11. Temperature distribution of air and water for a smooth tube.

From the air side, the finned tube gives more heat than the smooth tube because the thermal horizontal space between the two tubes of the cold fluid of the smooth tube is more than that in a finned tube. All the above-named integral finned tubes were noted to indicate that the superior model that would yield the maximum heat transfer rate is P = 1.6 mm. Also, the temperature is high at the entrance and begins to gradually decrease at the exit of the tube. The airflow through the tubes, as it is more turbulent in the model, is P = 1.6 mm.

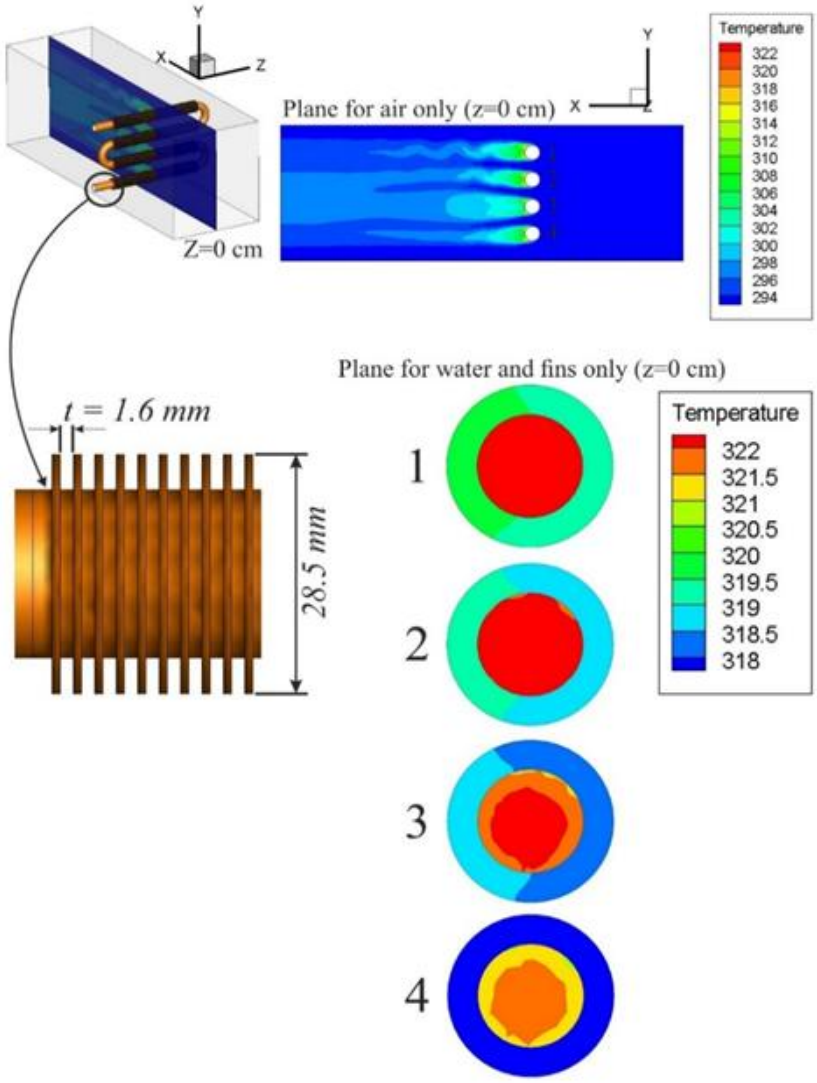

Fig. 12. Temperature distribution of air and water for the test tube with pitch ratio 1.6 mm, where 1, 2, 3, and 4 indicate the cross-section of the upper, middle, and lower pass find tube, respectively.

It has been observed that the airspeed will vary between the inlet and the section after the test tubes because in the inlet part, the airflow will be narrowing between the section at the test tubes, and this will create turbulence and eddies in the airflow behind the tube. The length and duration of this turbulence a relation to the distance between the tubes.

The higher the concentration of fin, the more turbulence will be present. The increase in the flow of the heating fluid increases the heat transfer rate and increases the turbulence in the flow. It is observed from all the above-mentioned integral finned tubes that the best temperature decrease is at the finned tube, P = 1.6 mm,

which increases the surface area of the heat exchanger, hence giving us the best model, and this is because of the increased effectiveness of the surface of a heat exchanger. The flow accelerated as fins act as an air originated, which in turn penetrates the adjacent thermal boundary layers. As a result, it increases the amount of thermal energy transferred.

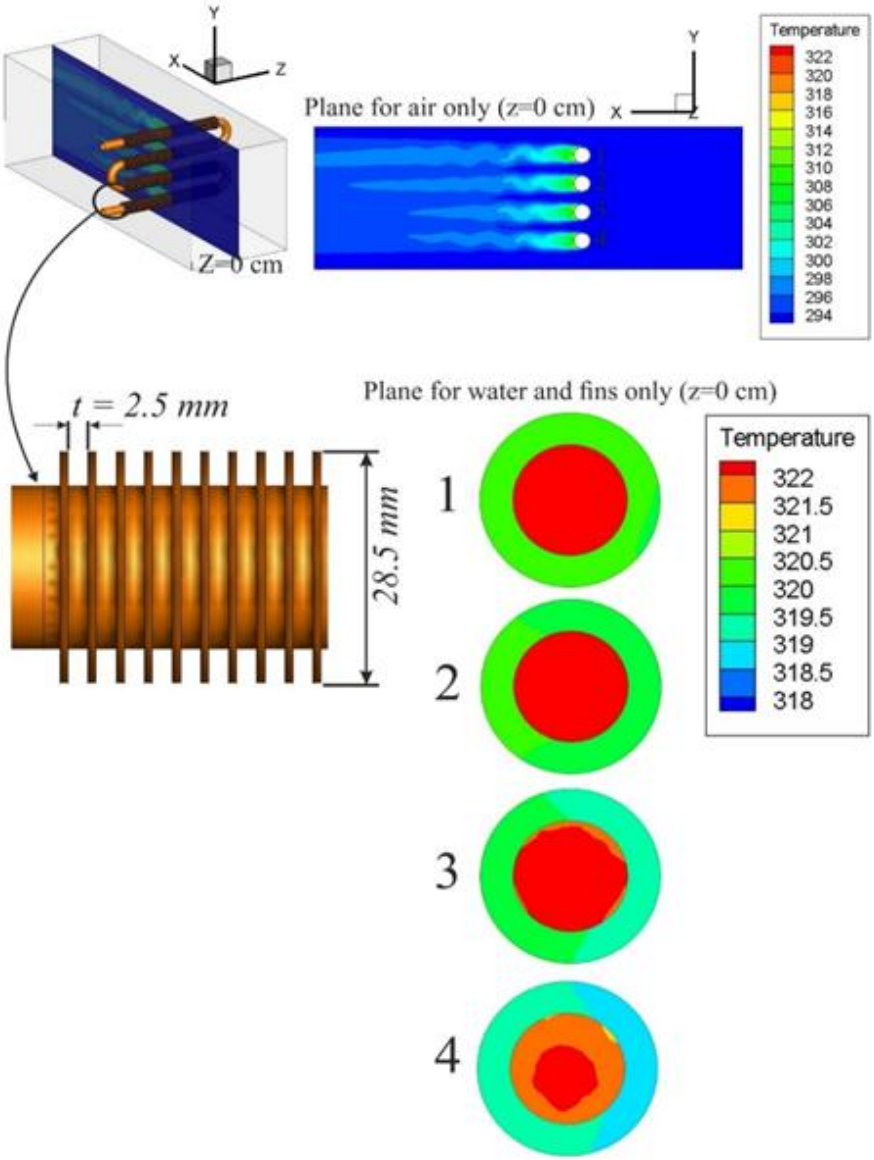

Fig. 13. Temperature distribution of air and water for the test tube with pitch ratio 2.5 mm, where 1, 2, 3, and 4 indicate the cross-section of the upper, middle, and lower pass find tube, respectively.

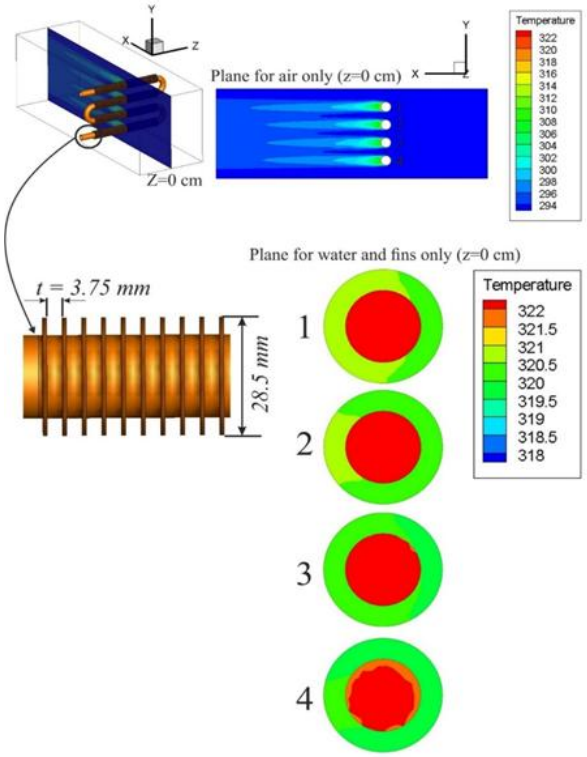

Fig. 14. Temperature distribution of air and water for the test tube with pitch ratio 3.75 mm, where 1, 2, 3, and 4 indicate the cross-section of the upper, middle, and lower pass find tube, respectively.

3.4. Pitch Ratio Effect on NTU

Figure 15 shows a relation between the number of transfer units and with Reynolds number for all simulated models due to the increase in the total heat transfer coefficient. The finned tube with a pitch of P = 1.6 mm gives a higher value of NTU than the others due to the increase in the surface area and the number of fins, as it works to direct the movement of air, which leads to an increase in thermal energy dissipation and Penetration of the thermal boundary layer.

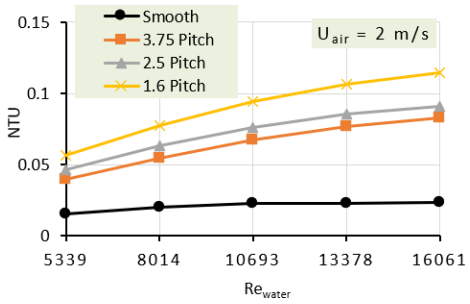

Fig. 15. Relationship between the number of transfer units (NTU) and the Reynolds number at constant velocity of air at 2 m/s.

4. Conclusions

This study numerically investigated the medium temperature integral finned tubes with variable pitches to get the optimum thermal performance of the heat exchanger. SolidWorks 2018 was used for the model's generation, and ANSYS Fluent 19R2 was used for the hydrothermal process simulation. In every case, the rate of heat transmission taking place between hot water to cold air in the finned tube is more than it happens in the case of a smooth tube. The specimen consisted of the fined tube with the ratio of the pitch P = 1.6, 2.5, and 3.75 mm that increases the rate of heat transfer by 74%, 68.9% and 63.3% respectively, compared to the smooth tube. The higher the rate of hot water flow, the smaller the range of water temperature.

The authors recommend future work as a continuation of the research by investigating the effect of different types of nanofluids and various types of fins.

Nomenclature

A_i	Tube area of internal surface, m^2
A_o	Tube area of external surface, m^2
C_p	Specific heat, J/kg·K
F	Correction factor
h_i	Interior side tube heat transfer coefficient, $W/m^2·K$
h_o	Exterior side tube heat transfer coefficient, $W/m^2·K$
m_w	Mass flow rate of water, kg/s
Nu_w	Nusselt number
Pr_w	Prandtl number
Re_w	Reynolds number
U_i	Overall heat transfer coefficient of interior side tube, $W/m^2·K$
U_w	air velocity, m/s

Greek Letters

Ɛ	Effectiveness
ρ	density, kg/m^3

Abbreviations

ER	Enhancement ratio
HVAC	Heating, ventilation, and air conditioning
LMTD	Logarithmic Mean Temperature Difference
NTU	Number of transfer units

References

1. Mon, M.S.; and Gross, U. (2004). Numerical study of fin-spacing effects in annular-finned tube heat exchangers. *International Journal of Heat and Mass Transfer*, 47(8-9), 1953-1964.
2. Hofmann, R.; Frasz, F.; and Ponweiser, K. (2007). Heat transfer and pressure drop performance comparison of finned-tube bundles in forced convection. *WSEAS Transactions of Heat Mass Transfer*, 2(4), 72-88.
3. Jung, D.; and Assanis, D.N. (2006). Numerical modeling of a crossflow compact heat exchanger with louvered fins using thermal resistance concept. *SAE Technical Paper*, 2006-01-0726.

4. Taher, F.A.Z. (2019). *Experimental and numerical study of integrated finned heat exchanger*. MSc Thesis, Wasit University, Iraq.
5. Wais, P. (2010). Fluid flow consideration in fin-tube heat exchanger optimisation. *Archives of Thermodynamics*, 31(3), 87-104.
6. Ismail, M.S.; Hassab, M.; and El-Maghlany, W.M. (2019). Comparative three-dimensional CFD study for inline crossflow plate finned tube heat exchanger. *Proceedings of the 4th World Congress on Momentum*, *Heat and Mass Transfer*. Rome, Italy, 23-56.
7. Merdan, S.H.; and Khalefa Kadhim, Z. (2020). Study the flow direction and number of tubes in crossflow heat exchanger to improve the heat transfer coefficient. *Proceedings of the 2nd International Scientific Conference of Engineering Sciences* (*ISCES* 2020), *IOP Conference Series: Materials Science and Engineering*, Diyala, Iraq.
8. Wais, P. (2016). Correlation and numerical study of heat transfer for single row crossflow heat exchangers with different fin thickness. *Procedia Engineering*, 15(7), 177-184.
9. Ravikumar, K.; Raju, C.N.; and Saheb, M. (2017). CFD Analysis of a crossflow heat exchanger with different fin thickness. *International Journal of Dynamics of Fluids*, 13(2), 345-362.
10. Taher, F.A.; and Kadhim, Z.K. (2019). Improvement of heat transfer coefficient for a cross flow heat exchanger by using the high integral finned tube. *Journal of University of Babylon for Engineering Sciences*, 27(3), 99-113.
11. Sahel, D.; Ameur, H.; and Mellal, M. (2020). Effect of tube shape on the performance of a fin and tube heat exchanger. *Journal of Mechanical Engineering and Sciences*, 14(2), 6709-6718.
12. Merdan; S.A.; Kadhim, Z.K.; and Alwan, A.A. (2020). CFD analysis for different types of fins to enhancement the heat transfer rate through a cross flow heat exchanger. *Proceedings of the 1st Conference on Science and Technology for Early Career Researchers and Postgraduate Students* (*STEPS* 2020), *IOP Conference Series: Materials Science and Engineering*, Erbil, Iraq.
13. Kadhim, Z.; Kassim, M.S.; and Hassan, A. (2016). Effect of integral finned tube on heat transfer characteristics for crossflow heat exchanger. *International Journal of Computer Applications*, 139(3), 20-25.
14. Kadhim, Z.K.; Kassim, M.S.; and Hassan, A.Y.A. (2016). CFD study for crossflow heat exchanger with integral finned tube. *International Journal of Scientific and Research Publications*, 6(6), 668-677.
15. Nuntaphan, A.; and Kiatsiriroat, T. (2004). Effect of fly ash deposit on thermal performance of spiral finned-tube heat exchanger under dehumidifying condition. *Songklanakarin Journal of Science and Technology*, 26(4), 509-519.
16. Habeeb, L.J.; Karamallah, A.A., Rahmah, A.M. (2015). Heat transfer analysis of integral-fin tubes. *Engineering and Technology*, 2(2), 23-34.
17. Versteeg, H.K.; and Malalasekera, W. (2007). *An introduction to computational fluid dynamics. The finite volume method*. Pearson Education Limited.
18. ANSYS, A.F.U.G. (2011). *Southpointe*, *275 Technology Drive*. Canonsburg, USA, 15317.

19. Jessam, A.R.; Al-Kayiem, H.H.; Nasif, M.S.; and Albuali, A.A.J. (2020). Experimental and numerical assessment on s-shaped diffuser performance with different turbulence intensity. *Proceedings of the 1st* International *Conference of Electromechanical Engineering and its Applications* (*ICEMEA*-2020). *IOP Conference Series: Materials Science and Engineering*, Baghdad, Iraq.